Commun., **37**, 988 (1972).
(53) A. Živný and J. Pouchlý, *J. Polym. Sci., Part A-2*, **10**, 1467 (1972).
(54) J. Pouchlý and A. Živný, *J. Polym. Sci., Part A-2*, **10**, 1481 (1972).
(55) E. F. Casassa, *Polym. J.*, **3**, 517 (1972).
(56) A. Rosenthal, *Macromolecules*, **5**, 310 (1972).
(57) C. Strazielle in "Light Scattering from Polymer Solutions", M. B. Huglin, Ed., Academic Press, London, 1972.
(58) H. Eisenberg, "Biological Macromolecules and Polyelectrolytes in Solution", Clarendon Press, 1976.
(59) P. Munk and M. E. Halbrook, *Macromolecules*, **9**, 568 (1976).
(60) S. G. Chu and P. Munk, *J. Polym. Sci., Polym. Phys. Ed.*, **15**, 1163 (1977).
(61) S. G. Chu and P. Munk, *Macromolecules*, **11**, 101 (1978).
(62) D. J. DeRosier, P. Munk, and D. J. Cox, *Anal. Biochem.*, **50**, 139 (1972).
(63) P. J. Flory, "Principles of Polymer Chemistry", Cornell University Press, Ithaca, N.Y., 1953.
(64) T. M. Aminabhavi, to be published.
(65) P. J. Flory and W. R. Krigbaum, *J. Chem. Phys.*, **18**, 1086 (1950).
(66) K. C. Chao and O. A. Hougen, *Chem. Eng. Sci.*, **7**, 246 (1958).
(67) R. Koningsveld, W. H. Stockmayer, J. W. Kennedy, and L. A. Kleintjens, *Macromolecules*, **7**, 73 (1974).

Viscoelastic Properties of Linear Polymers with High Molecular Weights and Sharp Molecular Weight Distributions

Yoshinobu Isono,* Teruo Fujimoto, Naoki Takeno, Hirokazu Kjiura,† and Mitsuru Nagasawa

Department of Synthetic Chemistry, Nagoya University, Chikusa-ku, Nagoya, Japan (Code 464). *Received September 21, 1977*

ABSTRACT: Viscoelastic properties of concentrated solutions of linear polystyrenes having high molecular weights and sharp molecuclar weight distributions were studied by a Weissenberg rheogoniometer and also by a torsional creep apparatus of the Plazek type. Dynamic modulus and creep compliance of those samples were determined as functions of frequency and time, respectively. It was confirmed that there are two different relaxation mechanisms in the viscoelastic behavior of concentrated solutions of linear polymers. The separation of two mechanisms appears clearer in this study than in other studies, due to the high molecular weights of our samples. Deviation from the WLF equation on the temperature dependence of shift factor was found at high temperatures.

It is generally accepted that viscoelastic properties of concentrated solutions and the melts of linear polymers are governed by two types of relaxation mechanisms: the intramolecular motions of segments and the molecular motions involving the adjustments and the shifting of chain entanglements.[1-3] The two mechanisms should have quite different characteristics and the relaxation times corresponding to the two mechanisms should be unrelated. That is, relaxation times involving intramolecular interactions are independent of molecular weight, whereas the relaxation times showing molecular motions depend on molecular weight.[6-9]

The presence of the two mechanisms can be observed as the appearance of the plateau region in the storage modulus vs. frequency plot or in the creep compliance vs. time plot. That is, a minimum is observed in the relaxation or retardation spectra.[4-9] These features are expected to become clearer with increasing molecular weight.

The purpose of this work is to study such viscoelastic properties of linear polymer solutions in the plateau and terminal zones, using the polystyrenes having high molecular weights and narrow molecular weight distributions.

Moreover, if these two relaxation mechanisms are separated enough, the temperature dependence of the shift factor for time–temperature superposition would not necessarily be the same in both regions, as was pointed out by Sōen, Ono, Yamashita, and Kawai.[10] Nevertheless, the shift factors reported in the literature were always well expressed by the WLF equation.[2] It is also our purpose to clarify this problem using samples having high molecular weights and narrow molecular weight distributions.

† Mitsui Petrochemical Industries, Ltd., Waki-cho, Kuga-gun, Yamaguchi-ken, Japan (Code 740).

Table I

sample no.	M_w	M_w/M_n	C, g/dL
201	1.4×10^6	1.02[a]	10.5
			20.9
			26.4
			102 (undiluted)
002	1.1×10^7		11.7
			15.8
			56.4
			72.0
			80.8
401	1.2×10^7		7.92
			15.5

[a] The values calculated from the molecular weight distribution curve determined by the sedimentation-velocity method.[11]

Experimental Section

Samples. Nearly monodisperse polystyrene samples were prepared by an anionic polymerization method as described in a previous paper.[11] Low and high molecular weight tails of these samples were removed by fractional precipitation from their benzene solutions with addition of methanol. Samples no. 002 and 401 have high molecular weights, while sample no. 201 has an ordinary molecular weight. The molecular weights of these samples are listed in Table I. The weight average molecular weights of the samples were determined by the light-scattering method in *trans*-decalin at 22 °C (Θ temperature) or 30 °C and in cyclohexane at 35 °C (Θ temperature) using a light-scattering photometer, Fica-50. The molecular weight distributions of the samples were checked by the sedimentation–velocity method in cyclohexane at 35 °C using an analytical ultracentrifuge, Beckmann Spinco Model E. The molecular weights of samples no. 002 and 401 were so high that it was difficult to determine their molecular weight distributions by the sedimentation–velocity method. At least, however, it may be concluded from the sedimentation patterns in Figure 1 that the molecular weight dis-

0024-9297/78/2211-0888$01.00/0 © 1978 American Chemical Society

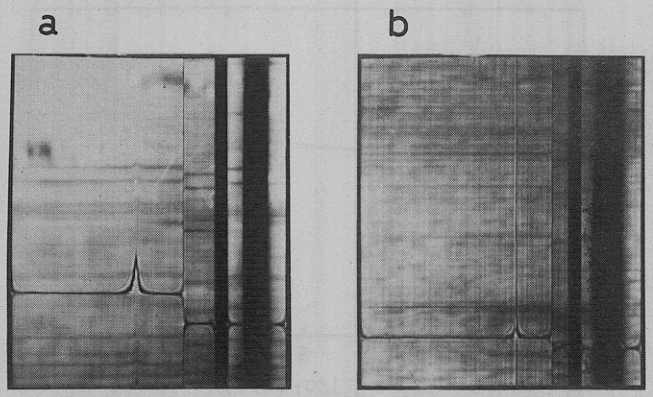

Figure 1. Examples of the sedimentation patterns of the samples: (a) Sample no. 002; solvent, cyclohexane; 35 °C; concentration 0.03 g/dL; speed of rotation, 42040 rpm; angle, 70°; time, 12 min. (b) Sample no. 401; solvent, cyclohexane; 35 °C; concentration 0.19 g/dL; speed of rotation, 25980 rpm; angle, 70°; time, 20 min.

tributions of the samples are sharp enough.

The solvent, benzyl *n*-butyl phthalate, was obtained from Tokyo Kasei Co. Ltd., and was purified by distillation at a reduced pressure (3.5×10^{-4} mmHg, 160 °C). The density and viscosity of the solvent were 1.111 g/mL and 38.7 cP at 30 °C, respectively.

The sample solutions for the Weissenberg Rheogoniometer were made up by weight and converted to C (g/dL) by assuming additivity of the specific volume of polymer and solvent. Cyclohexane or dichloromethane was added to accelerate the dissolution of the samples into benzyl *n*-butyl phthalate and, later, removed by evaporation under high vacuum. To prepare the solutions, the vessels were very gently shaken by hand once a day at 50 °C to avoid mechanical degradation of the high molecular weight samples. The concentrations of the samples studied here are also listed in Table I.

Disk-shaped samples for creep measurement were formed in stainless steel molds: The polystyrene sample was dissolved into a mixture of benzyl *n*-butyl phthalate and dichloromethane and the solution was spread on a glass plate floating on mercury at room temperature. By evaporating dichloromethane, the mixture of benzyl *n*-butyl phthalate and polystyrene was cast into thin films of about 0.2 mm thickness. The films thus formed were further dried in a vacuum oven. The oven temperature was raised gradually from room temperature to about 110 °C, kept at the temperature for at least 12 h, and then gradually lowered to room temperature. Circular films with a desired diameter were cut from the thin film and were placed between stainless steel plates in a stainless steel mold. The plates employed for the creep measurement were coated by the same samples as previously, using its dilute benzene solution. With this precoating of the plates, the use of an adhesive agent between the plates and sample could be avoided. In our preliminary experiments, we found somewhat poor reproducibility in creep measurements if an adhesive agent was used. This poor reproducibility may be caused by the contribution of the adhesive agent to creep compliance of the sample and/or by degradation of this agent at high temperatures.

The plates and the mold were designed to fit together well. The mold was gradually heated in a vacuum oven to about 160–200 °C, depending on the polymer concentration. The adhesion between the sample disk and the stainless steel plates was satisfactory, when the temperature was returned to room temperature. Solvent loss during this process was shown to be negligible. Measurement of the limiting viscosity numbers of the samples showed that no degradation had occurred. The disk samples sandwiched between the two stainless steel plates were placed in the torsional creep apparatus. The centering of the piano wire, the supporting rod, and the plates was carefully done before the disk samples were installed.

Measurements. A Weissenberg rheogoniometer, type R-17, manufactured by Sangamo Controls Ltd., was used to measure the complex modulus. It is a cone-and-plate viscometer with a facility for normal force measurement and with a magnetic expander as a gap-servo system. The frequency of the oscillations ranged from 9.8×10^{-1} to 9.8×10^{-3} rad/s. The temperature ranged from 10 to 100 °C with accuracy of ±0.1 °C. In the present work, a platen of 5 cm diameter and 4° angle was used with a torsion bar of 2 or 4 mm diameter. The details and reliability of the Weissenberg rheogoniometer, type R-17, were reported previously.[12,13] It was confirmed that the experimental results do not depend on the amplitude of oscillation.

The torsional creep apparatus, which is similar to one described by Plazek,[14] was used to measure the creep compliance. A piano wire with 1 mm diameter and 120 cm length was used as a torsion wire. The diameters of the disk samples were 10, 13, 17, and 22 mm. The sample chamber was made of Pyrex glass and immersed in a silicon oil bath. The thickness of the disks, in the range between 2 and 8 mm, was frequently measured with a cathetometer to a precision of 0.05 mm. No detectable change in the thickness of the sample disk was found.

Argon gas was passed through a copper tube in an oil bath and into the sample chamber. An electrical heater was placed around the supporting rod to prevent the leakage of heat through the rod. The supporting rod was made of Micalex, manufactured by Tokyo Shibaura Electric Co. Ltd., which is a poor conductor of heat and a hard solid (tensile strength 400–450 Kg/cm^2, with a compressive strength of 1800–2000 Kg/cm^2, a bending strength of 800–1000 Kg/cm^2, and heat resistance to 500 °C). The difference between the temperature of the oil bath and that of the air was within ±0.1 °C. It was also preliminarily confirmed that the temperature difference between the stainless steel plates and the air inside the sample chamber was negligible.

The torsional angle of the sample disk was measured to a precision of 0.01° by recording the angular deflection of a laser light beam reflected from a mirror fixed near the torsion axis. The reflection of light was detected with phototransistors placed at the interval of 0.5°. The measurements began 5 s after the start of creep.

The creep compliance $J(t)$ was calculated from the equation

$$J(t) = \frac{\pi r^4}{2hk\Theta}\theta(t)$$

where r and h are the radius and height of the sample disk, respectively, $k\Theta$ is the torque given to the sample with a piano wire, and $\theta(t)$ is the angle of the upper plate recorded as a function of time.

Results and Discussion

Examples of the change in creep compliance (J) with time and of change in storage modulus (G') with frequency are shown in Figures 2 and 3, respectively. All data at various temperatures are shifted on the curve at a reference temperature, 100 °C, assuming the time–temperature superposition principle. Since slight vertical shifts were required in the superposition procedure, we employed the method of Plazek.[15] That is the horizontal shift factors (time scale shift factors, log a_T) were first determined from the superposition of d log $J(t)$/d log t vs. log t curves at individual temperatures in the case of creep compliance and from that of tan δ ($= G''/G'$) vs. log ω curves in the case of complex modulus. Next, the vertical shifts were performed. Alternatively, we tried the superposition by the conventional method of Ferry,[2] i.e., by assuming that the vertical shift is only due to the rubber-elastic nature and the change in density with temperature. The difference between log a_T determined by two methods was about 0.5 at maximum. However, the difference gives no effect on the conclusions in this paper.

The creep compliance (J) master curve for the undiluted state of sample no. 201 with a lower molecular weight is shown in Figure 4. The storage modulus (G') and loss modulus (G'') master curves for the same sample are shown in Figure 5. Note that the plateau regions in J and G' master curves of Figures 4 and 5 have finite slopes and the maxima in G'' master curves are not clear.

The J master curves for solutions of sample no. 002 with high molecular weight are shown in Figure 6. The creep experiments for the undiluted state of sample no. 002 were

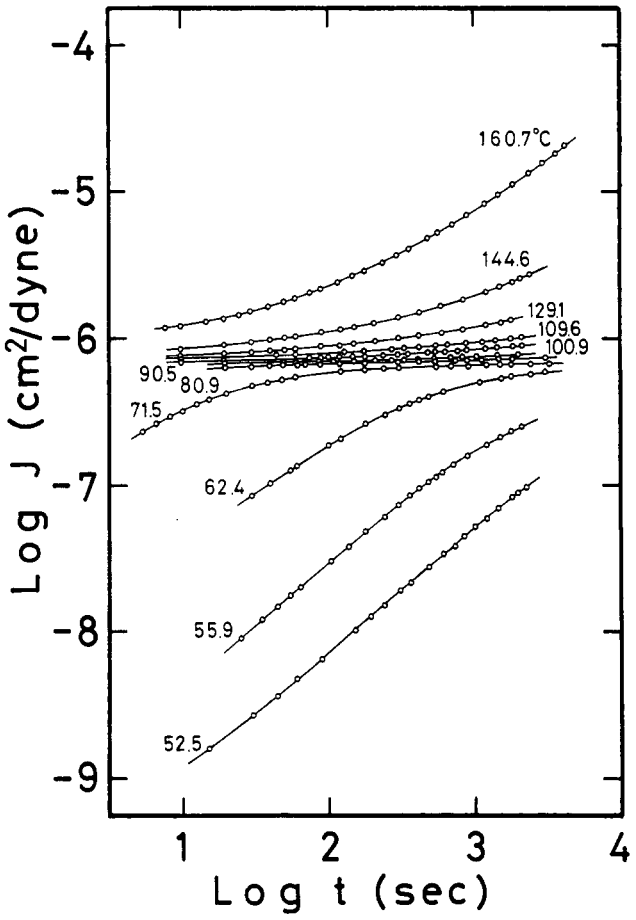

Figure 2. Experimental creep compliance plotted double logarithmically against time at various temperatures (sample no. 002; concentration 80.8 g/dL).

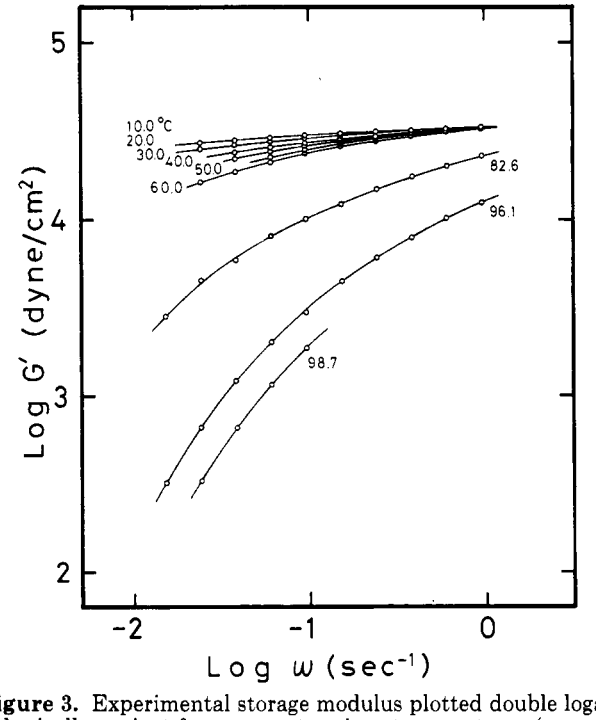

Figure 3. Experimental storage modulus plotted double logarithmically against frequency at various temperatures (sample no. 401; concentration 15.5 g/dL).

not carried out in order to avoid degradation of the sample. The G' and G'' master curves for solutions of samples no. 002 and 401 are shown in Figure 7. In the J curves of Figure 6, the flow regions shift strongly to the long time

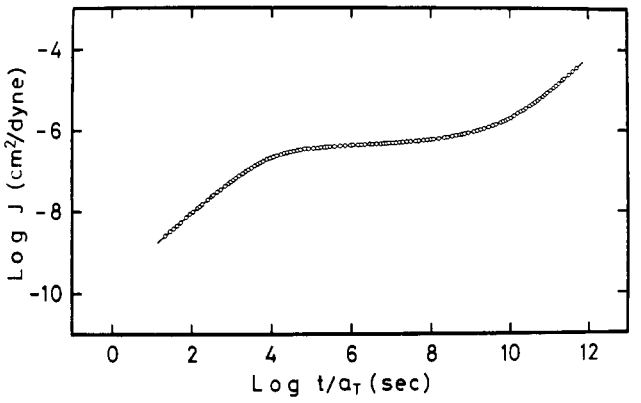

Figure 4. Creep compliance master curve for sample no. 201: concentration 102 g/dL (undiluted); temperature 100 °C.

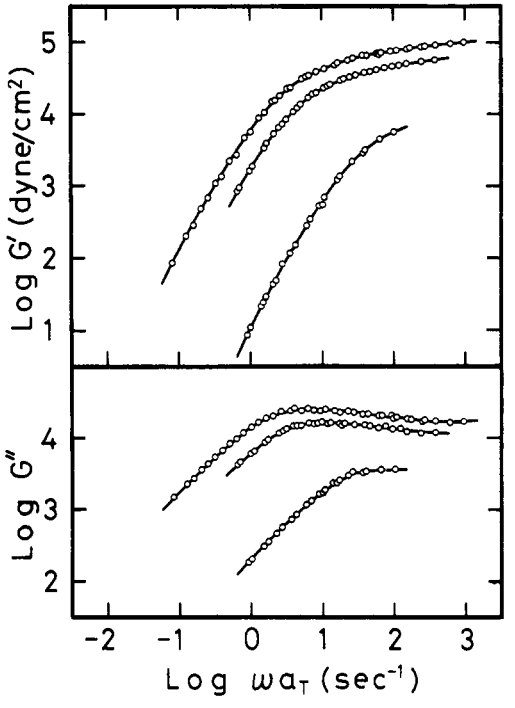

Figure 5. Storage and loss modulus master curves for sample no. 201 at various concentrations. Concentrations are 10.5, 20.9, and 26.4 g/dL from bottom to top, respectively (temperature 100 °C).

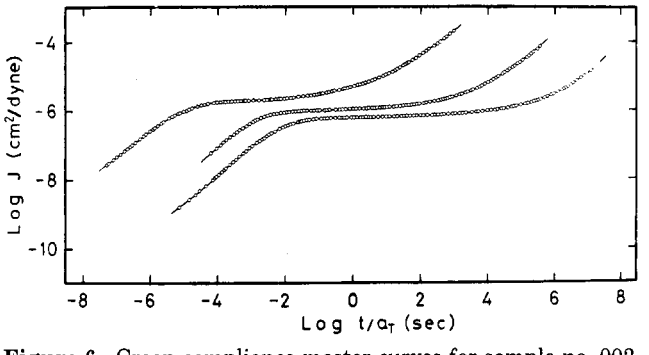

Figure 6. Creep compliance master curves for sample no. 002 at various concentrations. Concentrations are 56.4, 70.2, and 80.8 g/dL from left to right, respectively (temperature 100 °C).

side, that is, the rubbery plateau regions exist over a very wide time scale and are almost flat. The plateau regions in the G' curves of Figure 7 are also more nearly horizontal than those of Figure 5 and the maxima in the G'' curves of Figure 7 are distinct even at low concentrations. The features pointed out above become clearer as the con-

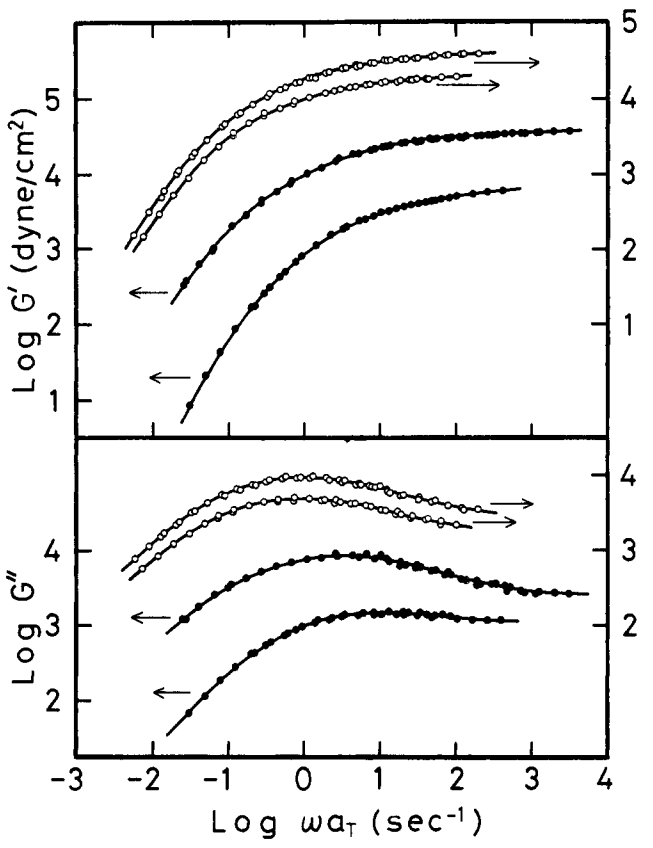

Figure 7. Storage and loss modulus master curves for samples no. 002 (○) and no. 401 (●) at various concentrations. Curves for sample no. 002 are shifted upward by a factor of 10 to avoid overlapping. Concentrations: (○) 15.8, 11.7 g/dL from left to right, (●) 15.5, 7.92 g/dL from left to right (temperature 100 °C).

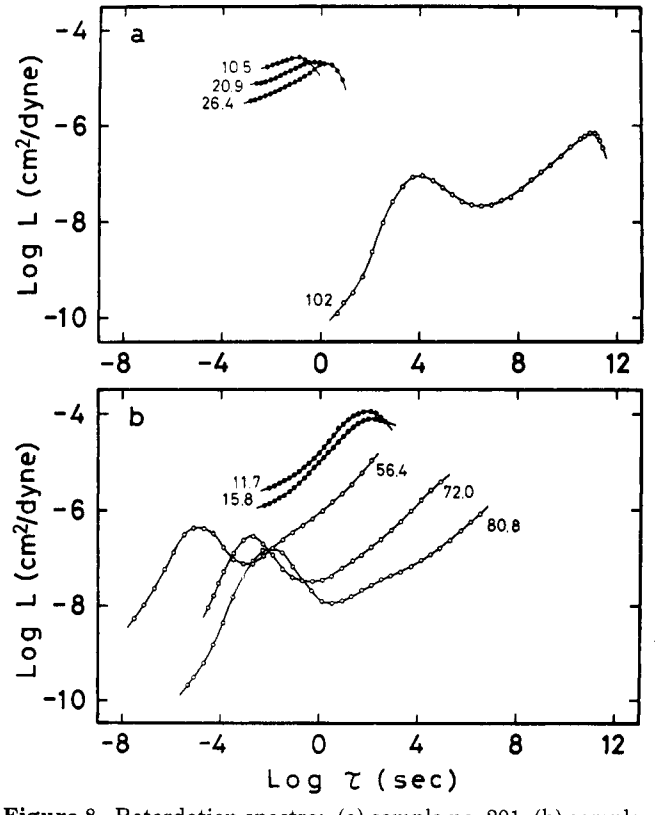

Figure 8. Retardation spectra: (a) sample no. 201, (b) sample no. 002. Concentrations (g/dL) are indicated in the figures. Open circles denote the retardation spectra calculated from $J(t)$, while filled circles denote the retardation spectra estimated from G' and G'' by the method described in the text.

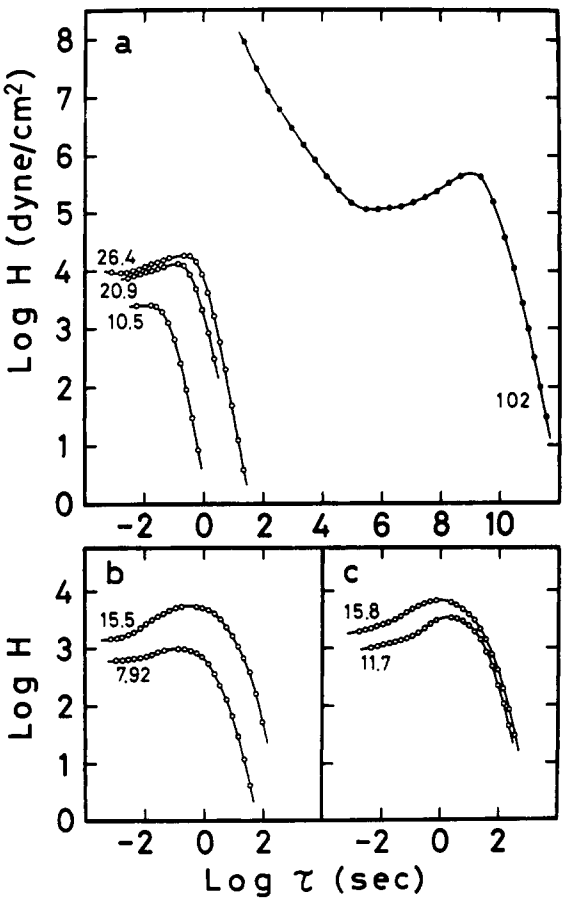

Figure 9. Relaxation spectra: (a) sample no. 201, (b) sample no. 401, (c) sample no. 002. Concentrations (g/dL) are indicated in the figures. Open circles denote the relaxation spectra calculated from $G'(\omega)$, while filled circles denote the relaxation spectrum estimated from $J(t)$ by the method described in the text.

centration increases. The curve for sample no. 002 at 15.8 g/dL and that for sample no. 401 at 15.5 g/dL in Figure 7 can satisfactorily be superposed if the abscissa is shifted by 0.67. The difference in the abscissa for the two almost identical samples arises from the difference of both samples in the behavior of log a_T around 100 °C. If a temperature below 60 °C is chosen as the reference temperature, the difference between the two curves disappears. Anyway, this difference is immaterial for the purpose of this paper.

The retardation spectra which are obtained from the J master curves of Figures 4 and 6 by using the second approximation method of Schwarzl and Sterverman[2] are shown in Figure 8. The relaxation spectra which are obtained from the G' master curves of Figures 5 and 7 by using the second approximation method of Tschoegl[2] are shown in Figure 9. Figures 8 and 9 show that, if the molecular weights are high enough, the minima in $L(\tau)$ and the maxima in $H(\tau)$, showing the separation of two mechanisms, are clear. Although the temperature could not be raised high enough to observe the whole range of molecular motion in $L(\tau)$ in Figure 8 and also could not be lowered enough to observe the segmental motion in $H(\tau)$ in Figure 9, the combination of these figures for $H(\tau)$ and $L(\tau)$ clearly shows the existence of the peaks corresponding to the two mechanisms.

For comparison, G' and G'' for samples no. 201 and 002 in Figures 5 and 7 are converted to J' and J'', from which the retardation spectra are calculated by using the second approximation method of Tschoegl.[2] Those retardation spectra are also shown by filled circles in Figure 8.

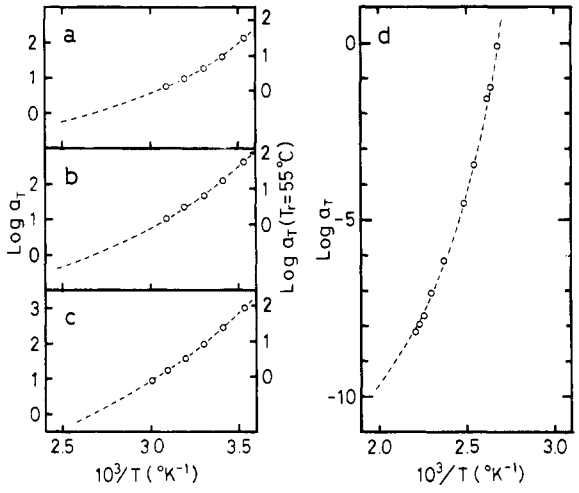

Figure 10. Temperature dependences of the shift factor for sample no. 201 at various concentrations. Reference temperature is 100 °C. Broken lines denote the WLF equations. Concentrations and the parameters in the WLF equations are listed in the following chart. The reference temperatures in the WLF equations were chosen arbitrarily.

	C, g/dL	T_r, °C	C_1	C_2
a	10.5	55	1.97	106
b	20.9	55	3.65	140
c	26.4	55	4.53	151
d	102	100	14.5	63.6

Moreover, the creep compliance J for sample no. 201 in Figure 4 is converted to J' and J'' by using the method of Shen and Jamison.[16] Then these J' and J'' are converted to G' and G'', from which the relaxation spectrum is calculated by using the method of Tschoegl. This relaxation spectrum is also shown by filled circles in Figure 9. In this conversion process from $J(t)$ to J' and J'', $J(t)$ in the glassy region was arbitrarily extrapolated. Therefore, $H(\tau)$ for undiluted sample no. 201 in Figure 9 cannot be discussed quantitatively.

These qualitative features of the retardation and relaxation spectra of monodisperse polymer can be observed in the experimental data of Ferry et al.,[4,5] Fujimoto et al.,[6] Masuda et al.,[8] Nemoto et al.,[9] and Riande et al.[17] Thus it is certain that two separate relaxation mechanisms corresponding to the segmental and molecular motions exist in the viscoelastic behavior of linear polymers. That is, the retardation and relaxation spectra of monodisperse polymers should have two peaks. However, the two mechanisms must overlap each other to some degree, if we take into account that the slopes in the plateau zones in Figures 6 and 7 are small but finite in spite of the high molecular weights of the samples. This may be due to the distribution of entanglement spacings.[2]

The shift factors a_T for sample no. 201 are plotted semilogarithmically against $1/T$ (where T is the absolute temperature) in Figure 10. They fit the WLF equation well (broken lines). Those for samples no. 002 and 401 with high molecular weights, shown in Figure 11, also fit the WLF equation well (broken lines) in the transition and rubbery regions, but a clear deviation from the WLF equation is observed in the higher temperature region at all concentrations. Moreover, the plots of Plazek,[18] that is, the plots log a_T vs. $(T - T_\infty)^{-1}$, where T_∞ is the temperature at which the free volume would disappear, are shown in Figure 12. In these plots, too, the linear relationship holds in the low temperature region, as was pointed out by Plazek,[18] but the shift factors clearly deviate from the straight lines in the higher temperature side. The

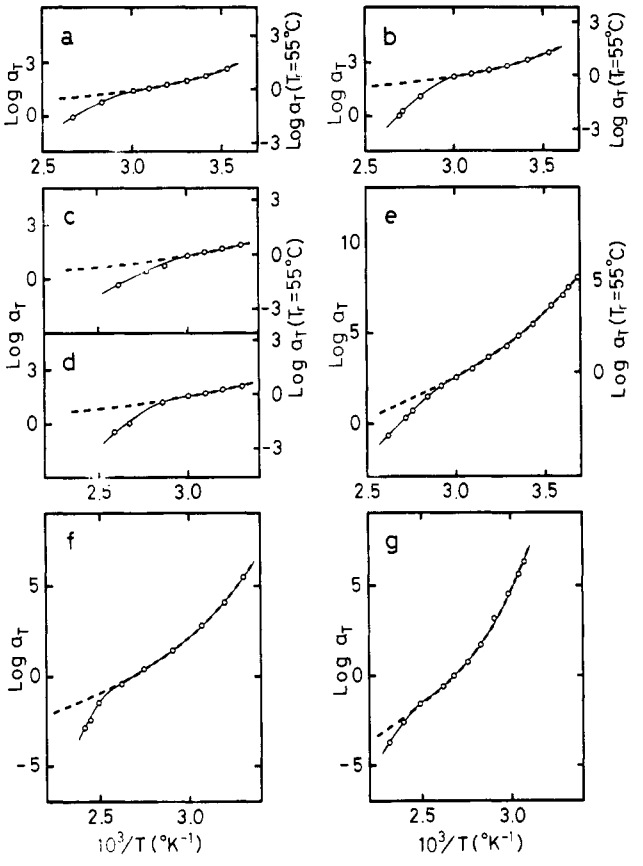

Figure 11. Temperature dependence of the shift factor for samples no. 002 and 401 at various concentrations. Reference temperature is 100 °C. Notations and others are the same as in Figure 10.

	sample no.	C g/dL	T_r, °C	C_1	C_2
a	401	7.92	55	1.42	99.7
b		15.5	55	1.79	109
c	002	11.7	55	1.67	112
d		15.8	55	1.95	117
e		56.4	55	7.06	133
f		72.0	100	6.19	150
g		80.8	100	8.55	111

errors in the values of a_T are large in the plateau region but, in any case, the errors are within the circles in the figures.

Instead of the WLF equation, Sōen et al. proposed the use of a few Arrhenius type equations with different activation energies, i.e., a combination of straight lines in log a_T vs. $1/T$ plots. However, the present data in Figures 10 and 11 cannot be expressed by such straight lines.

At the lower temperature side, the shift factor may be represented by the ratio of the local viscosities governing the segmental motion at the reference and measurement temperatures. And the local viscosity depends on the free volume. Therefore its temperature dependence may be expressed by the WLF equation. However, at the higher temperature side, the shift factor may be determined by the ratio of steady viscosities at two temperatures as was discussed by Markovitz.[19] There are two factors which determined the temperature dependence of the steady viscosity in concentrated solutions. One is the temperature dependence of the probability that vacant sites necessary for flow of segment are formed. The other is the temperature dependence of the probability that the molecule gains an energy enough to overcome the attractive force of segments at entanglement points. The latter energy depends on the number of entanglements per molecule N_E.

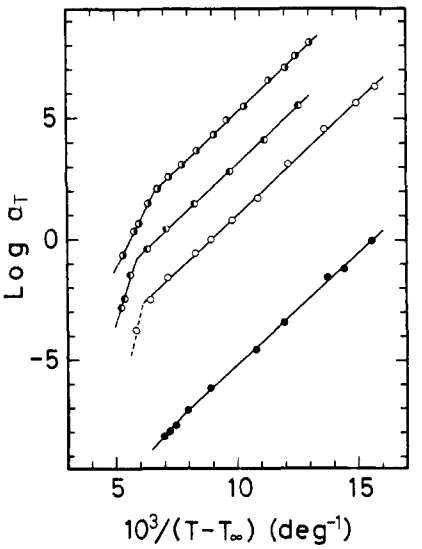

Figure 12. Shift factor a_T plotted semilogarithmically against $10^3/(T - T_\infty)$ for samples no. 201 and 002.

symbol	sample no.	C, g/dL	T_∞, °C
●	201	102	36.4
◑	002	56.4	-78.2
◐		72.0	-49.8
○		80.8	-10.8

The temperature dependence of the former probability may be similar to that of the WLF equation. Therefore if N_E is small, the shift factor may be expressed by the WLF equation, but it cannot always be true for high molecular weight samples.

Finally, the pseudo-equilibrium modulus of the entanglement network G^0_{eN}, which characterizes the rubbery plateau region, can be evaluated from the graphical integration of $G''(\omega)$ vs. ln ω and $H(\tau)$ or $L(\tau)$ vs. ln τ curves

$$G^0_{eN} = \frac{2}{\pi}\int_{-\infty}^{a} G''(\omega)\, d\ln\omega = \int_{a'}^{\infty} H(\tau)\, d\ln\tau = \left(\int_{-\infty}^{b} L(\tau)\, d\ln\tau\right)^{-1}$$

where a, a', and b are taken to encompass the maximum of $G''(\omega)$, $H(\tau)$, or $L(\tau)$.

The values of G^0_{eN} are plotted against the concentration of the sample in Figure 13. These values are found to be in good agreement with the values estimated from the horizontal heights in log G' vs. log ω and in log J vs. log t plots (Figures 6 and 7). The rubbery plateau regions are clear in these experiments. This agreement confirms the reliability of the present time–temperature superposition procedure, that is, the reliability of the estimated shift factors. Moreover, it is evident in Figure 13 that a linear relationship holds between log G^0_{eN} and log C, and the slope is 2.2–2.3. It is also clear that G^0_{eN} is independent of molecular weight up to 1.2×10^7 in agreement with previous work.[7,20,21] The average molecular weight between entanglement coupling loci M_e in the undiluted polystyrene is 1.26×10^4 if it is evaluated from the data in Figure 13, using the following equation.[2]

$$M_e = CRT/G^0_{eN}$$

Note Added in Proof: After submitting this paper for publication, we became aware of a similar study of

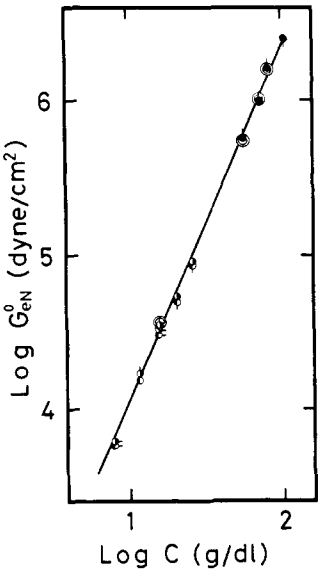

Figure 13. Concentration dependence of pseudoequilibrium modulus G^0_{eN} at 100 °C. Pip up, pip right, and pip down denote the data for samples no. 002, 401, and 201, respectively. Symbols ●, ◐, ◑, and also ⊛ denote the values evaluated from $L(\tau)$, $H(\tau)$, $G''(\omega)$, and also from heights of the rubbery plateau regions of $G'(\omega)$ or $J(t)$, respectively.

polystyrene ($M_w = 7.1 \times 10^6$ and 4.4×10^7) by Raghupathi.[22] Experimental results in the work are similar to those in the present work, but a difference is found in the behavior of shift factors. In his work, all shift factors fit a WLF equation.

References and Notes

(1) A. V. Tobolsky, "Properties and Structure of Polymers", Wiley, New York, N.Y., 1960.
(2) J. D. Ferry, "Viscoelastic Properties of Polymers", 2nd ed, Wiley, New York, N.Y., 1970.
(3) W. W. Graessley, *Adv. Polym. Sci.*, **16**, 1 (1974).
(4) W. Dannhauser, W. C. Child, Jr., and J. D. Ferry, *J. Colloid Sci.*, **13**, 103 (1958).
(5) J. W. Berge, P. R. Saunders, and J. D. Ferry, *J. Colloid Sci.*, **14**, 135 (1959).
(6) T. Fujimoto, N. Ozaki, and M. Nagasawa, *J. Polym. Sci., Part A-2*, **6**, 129 (1968).
(7) S. Onogi, T. Masuda, and K. Kitagawa, *Macromolecules*, **3**, 109 (1970).
(8) T. Masuda, K. Kitagawa, and S. Onogi, *Macromolecules*, **3**, 116 (1970).
(9) N. Nemoto, *Polym. J.*, **1**, 485 (1970).
(10) T. Soen, T. Ono, K. Yamashita, and H. Kawai, *Kolloid Z. Z. Polym.*, **250**, 459 (1972).
(11) T. Fujimoto and M. Nagasawa, *Polym. J.*, **7**, 397 (1975).
(12) H. Endo and M. Nagasawa, *J. Polym. Sci., Part A-2*, **8**, 371 (1970).
(13) H. Kajiura, H. Endo, and M. Nagasawa, *J. Polym. Sci., Part A-2*, **11**, 2317 (1973).
(14) D. J. Plazek, M. N. Vrancken, and H. W. Berge, *Trans. Soc. Rheol.*, **2**, 39 (1958).
(15) D. J. Plazek and A. J. Chelko, Jr., *Polymer*, **18**, 15 (1977).
(16) M. Shen and R. T. Jamison, *J. Polym. Sci., Part C*, **35**, 23 (1971).
(17) E. Riande, H. Markovitz, D. J. Plazek, and N. Raghupathi, *J. Polym. Sci., Poly. Symp.*, **No. 50**, 405 (1975).
(18) D. J. Plazek and V. M. O'Rourke, *J. Polym. Sci., Part A-2*, **9**, 209 (1971).
(19) H. Markovitz, *J. Polym. Sci., Polym. Symp.*, **No. 50**, 431 (1975).
(20) N. Nemoto, M. Moriwaki, H. Odani, and M. Kurata, *Macromolecules*, **4**, 215 (1971).
(21) Y. Einaga, K. Osaki, M. Kurato, and M. Tamura, *Macromolecules*, **5**, 635 (1972).
(22) N. Raghupathi, Ph.D. Thesis, University of Pittsburgh, 1975.